Primary familial brain calcification linked to deletion of 5' noncoding region of *SLC20A2*

Short title: PFBC due to partial deletion of *SLC20A2*

Petra Pasanen[1,2], Jussi Mäkinen[3], Liisa Myllykangas[4], Rita Guerreiro[5], Jose Bras[5], Miko Valori[6], Matti Viitanen[7,8], Marc Baumann[9], Pentti J. Tienari[6,10], Minna Pöyhönen[11], and Peter Baumann[12]

[1] Department of Medical Biochemistry and Genetics, University of Turku, Turku, Finland
[2] Tyks Microbiology and Genetics, Department of Medical Genetics, Turku University Hospital, Turku, Finland
[3] Department of Neurology, Tampere University Hospital, Tampere, Finland
[4] Department of Pathology, University of Helsinki and HUSLAB, Helsinki, Finland
[5] Department of Molecular Neuroscience, UCL Institute of Neurology, London, UK and Department of Medical Sciences and Institute of Biomedicine – iBiMED, University of Aveiro, 3810-193 Aveiro, Portugal
[6] Research Programs Unit, Molecular Neurology, University of Helsinki, Helsinki, Finland
[7] Department of Geriatrics, University of Turku, Turku, Finland
[8] Department of Neurobiology, Care Sciences and Society, Karolinska Institutet, Stockholm, Sweden
[9] Biochemistry/Developmental Biology, Meilahti Clinical Proteomics Core Facility, University of Helsinki, Helsinki, Finland
[10] Clinical Neurosciences, Neurology, University of Helsinki and Helsinki University Hospital, Helsinki, Finland
[11] Department of Clinical Genetics, Helsinki University Central Hospital and Department of Medical Genetics, University of Helsinki, Helsinki
[12] Department of Neurology and Clinical Neurophysiology, Lapland Central Hospital, Rovaniemi, Finland

Corresponding author:

Petra Pasanen
Institute of Biomedicine, Department of Medical Biochemistry and Genetics, University of Turku, Kiinamyllynkatu 10, FIN-20520 Turku, Finland
Tel.: +358 2 333 7456
Fax: +358 2 230 1280
e-mail: petra.pasanen@utu.fi

Abstract

Objectives

Primary familial brain calcification (PFBC) is a rare neurological disease often inherited as a dominant trait. Mutations in four genes (*SLC20A2*, *PDGFB*, *PDGFRB*, and *XPR1*) have been reported in PFBC patients. Of these, point mutations or small deletions in *SLC20A2* are most common. Thus far, only one large deletion covering entire *SLC20A2* and several smaller, exonic deletions of *SLC20A2* have been reported. The aim of this study was to identify the causative gene defect in a Finnish PFBC family with three affected patients.

Materials and methods

A Finnish family with three PFBC patients and five unaffected subjects was studied. Sanger sequencing was used to exclude mutations in the coding and splice site regions of *SLC20A2*, *PDGFRB* and *PDGFB*. Whole-exome (WES) and whole-genome sequencing (WGS) were performed to identify the causative mutation. A SNP array was used in segregation analysis.

Results

Copy number analysis of the WGS data revealed a heterozygous deletion of ~578 kb on chromosome 8. The deletion removes the 5' UTR region, the noncoding exon 1 and the putative promoter region of *SLC20A2* as well as the coding regions of six other genes.

Conclusions

Our results support haploinsufficiency of *SLC20A2* as a pathogenetic mechanism in PFBC. Analysis of copy number variations (CNVs) is emerging as a crucial step in the molecular genetic diagnostics of PFBC, and it should not be limited to coding regions, as causative variants may reside in the noncoding parts of known disease-associated genes.

Key words

deletion; primary familial brain calcification; promoter; *SLC20A2*

WORD COUNT OF THE ABSTRACT: 243

Primary familial brain calcification linked to deletion of 5' noncoding region of *SLC20A2*

Introduction

Primary familial brain calcification (PFBC, also previously known as idiopathic basal ganglia calcification, IBGC, or Fahr's disease) is a rare neurological disorder with a variable phenotype. The disease onset is usually between 30 and 50 years and the typical symptoms include both movement disorders (parkinsonism, dystonia, ataxia, chorea) and neuropsychiatric disturbances such as psychosis, dementia and frontal or subcortical cognitive dysfunction. The typical findings, bilateral and symmetric hydroxyapatite deposits, are seen in basal ganglia, dentate nuclei and thalamus in patients with normal serum levels of calcium, phosphate, alkaline phosphatase, and parathyroid hormone. However, variation in the clinical manifestations is common even within families, and asymptomatic individuals with calcifications have been reported (1-3).

PFBC is often inherited as a dominant trait. The first causative gene, *SLC20A2*, was reported in 2012 by Wang et al. (2) Since the original report, many other studies have confirmed that mutations in this gene account for up to 40 to 50 % of PFBC (4, 5). The other causative genes are *PDGFRB* on 5q32 (6), *PDGFB* on 22q13.1 (7) and *XPR1* on 1q25.1 (8).

SLC20A2 codes for an inorganic phosphate (Pi) transporter, PiT-2 that also functions as a retroviral receptor (9-11). Mutations in *SLC20A2* result in impaired phosphate transport and accumulation of phosphate in the extracellular matrix in the affected brain regions (2, 12). Functional studies suggest that the deleterious consequences of *SLC20A2* mutations are due to haploinsufficiency rather than dominant-negative effects (2). Studies on *Slc20a2* knock-out mice have shown that PiT-2 also has an important role in maintaining the normal low level of Pi in the cerebrospinal fluid (CSF) (13). Jensen et al. hypothesized that increased CSF Pi concentration due to defective PiT-2 could lead to pericyte transformation to a mineralizing

cell type and thus calcification of blood vessels (13). Another disease mechanism is proposed by the functions of *PDGFRB* and *PDGFB* which code for the platelet-derived growth factor receptor β and its ligand, platelet-derived growth factor β, respectively. Mutations in both *Pdgfb* and *Pdgfrb* have been linked to pericyte decifiency and impaired blood-brain barrier (BBB) integrity in mouse models (14, 15), which might lead to accumulation of calcium deposits in the brain (6, 7). The protein coded by *XPR1* is a retroviral receptor that has been shown to mediate phosphate export (16). Mutations in *XPR1* inhibit phosphate export and are likely to result in increased concentrations of intracellular phosphate (8). This might lead to decreased PiT-2-driven Pi uptake from the CSF, resulting in elevated CSF Pi concentration, as hypothesized by Jensen et al. (13).

Pathogenic *SLC20A2* mutations are typically missense (4, 5, 17-24) and nonsense mutations (4, 17, 25, 26), small deletions (2, 4, 5, 17, 19-21, 27-30) or splice site mutations (4, 5, 19). Two studies have broadened the mutational spectrum of *SLC20A2*: In 2014, a large deletion encompassing the entire coding region of *SLC20A2* was reported (25). In a recent study by David and coworkers, smaller deletions covering exon 2, exon 4 and exons 4 and 5 of *SLC20A2* were found in four patients in a cohort of 24 PFBC patients (31). Thus, analysis of copy number variations (CNVs) is emerging as a crucial step in molecular genetic diagnostics of PFBC.

Here we report a novel heterozygous deletion covering the 5' UTR and most likely the promoter region of *SLC20A2* and extending up to *FNTA*. The mutation segregates with PFBC in a Finnish family with three affected subjects. To our knowledge, this is the first report of a Finnish family with PFBC and the first *SLC20A2* mutation in the noncoding region.

Materials and methods

Subjects

We studied a PFBC family with three affected patients, the proband (II:2), his sister (II:5) and daughter (III:1). The inheritance pattern was consistent with autosomal dominant disease. The pedigree of the family is shown in Figure 1b. All patients were clinically examined at the Lapland central hospital. Two affected patients and five unaffected persons from the family were recruited for the study. No DNA from the deceased patient (II:2) was available for genetic testing. The study was approved by the Ethics Committee of Oulu University Hospital. Informed consent was obtained from all individual participants included in the study.

The proband, II:2, presented with symmetrical blepharospasm and bilateral facial spasm at the age of 66 years. Botulinumtoxin A injection treatment had only minor effect on the spasms. No additional findings were noted in clinical neurological examination. Brain magnetic resonance imaging (MRI) and computed tomography (CT) studies showed bilateral calcifications in basal ganglia and cerebellum (Figure 1a). Lowered perfusion in these brain areas was also noted in single positron emission tomography (SPECT) examination. The patient died of prostate cancer at the age of 69 years.

Patient II:5 had motor deficits, balance problems and memory disturbance. Clinical neurological examination was performed at 70 years. The patient had slight apraxia, mild balance impairment and lower limb ataxia but no dystonic movements. Mini Mental State Examination (MMSE) score was 19/30 consistent with mild dementia. Brain CT showed

146 calcifications in corona radiata and in cerebellum, anterior to lateral ventricles and vascular
147 degeneration. No hippocampal atrophy was seen.

148

149 The third affected patient, III:1, was diagnosed with torticollis spasmodica at the age of 29
150 years. She responded well to botulinumtoxin A injection treatment. Brain MRI showed
151 bilateral calcifications in the basal ganglia, thalamus and nucleus dentatus.

152

153 Serum levels of calcium, phosphate, alkaline phosphatase and parathyroid hormone were
154 normal in all three patients.

155

156 **Genetic methods**

157 DNA was extracted from peripheral EDTA blood with the Illustra Nucleon BACC3 Genomic
158 DNA Extraction Kit (GEHealthcare, Little Chalfont, Buckinghamshire, UK). The coding
159 regions and flanking intronic splice sites of *SLC20A2* (NM_006749.4), *PDGFRB*
160 (NM_002609.3) and *PDGFB* (NM_002608.3) were amplified by PCR and sequenced in both
161 directions using the BigDye Terminator v3.1 Cycle Sequencing Kit (Applied Biosystems,
162 CA, USA).

163 Whole exome sequencing (WES) of the two affected patients and one unaffected subject was
164 performed by the Institute for Molecular Medicine Finland (FIMM, University of Helsinki,
165 Finland). Exome enrichement was done using the SeqCap EZ Human Exome Library v3.0
166 (Roche Nimblegen, Basel, Switzerland) and the resulting libraries were sequenced on the
167 Illumina HiSEQ platform (Illumina, San Diego, CA, USA) to a mean target coverage of
168 58.8x (II:5), 62.4x (III:1), and 31.3x (III:2). Sequences were aligned to GRCh37/hg19,

variants called using the variant calling pipeline (vcp) developed at FIMM and the resulting variants were annotated with ANNOVAR(32).

Whole genome sequencing (WGS) of one affected and one unaffected subject was done by NGI Sweden (The National Genomics Infrastructure, Science for Life Laboratory, Solna, Sweden). Libraries were prepared using the TruSeq DNA PCR-free kit and sequenced on a HiSeq X Platform (Illumina, San Diego, CA, USA) to a mean coverage of 41.78x (III:1) and 41.75x (III:2). Sequences were aligned to GRCh37/hg19. Variant calling pipeline followed the GATK best practice guidelines. Small indels and SNVs were annotated with SnpEff(33) and ANNOVAR. Structural variants and larger copy number variants were identified by cn.mops(34) and Manta (https://github.com/Illumina/manta).

Additionally, five samples (II:3, II:4, II:5, II:6, II:7) were genotyped using genome-wide SNP array, the HumanOmniExpress Bead chip (Illumina, San Diego, USA).

Results

Sanger sequencing ruled out coding and splice site mutations in *SLC20A2*, *PDGFRB* and *PDGFB*. Exome sequencing did not result in any potentially causative variants shared by the two affected patients. Copy number analysis of the WGS data (subject III:1) revealed a heterozygous deletion of 578,164 bp on chromosome 8 (genomic coordinates chr8: 42,338,721 - 42,916,885) (Supporting table 1, Supporting figure 1). The deletion was also visible in the SNP array data (subject II:5) with breakpoints at rs11780448 (chr 8: 42,325,328) and rs13248091 (chr8: 42,929,226 bp) (Supporting figure 2). The unaffected subject III:2 did not have the deletion based on WGS (Supporting table 1, Supporting figure 1).

The deletion removes the noncoding exon 1, 5' UTR region and the putative promoter region of *SLC20A2* as well as the whole coding regions of six other genes (*SMIM19*, *CHRNB3*, *CHRNA6*, *THAP1*, *RNF170*, and *HOOK3*). The other deletion breakpoint is located between second and third exon of *FNTA*.

In order to test whether the deletion segregates with PFBC in this family, we genotyped additional four unaffected family members on a SNP array. The combination of WGS and SNP array data showed complete segregation of the deletion with the disease: the deletion was found in the two affected family members from whom DNA was available for testing, and was absent in the five unaffected relatives (Figure 1b, Supporting figure 2).

Discussion

Large deletions in causative genes for PFBC have been described in a few families. The first causative large copy number variant (CNV) for PFBC was reported by Baker el al. in a Canadian family (25). A partial deletion of *PDGFB* was subsequently described by Nicolas et al. (35). Recently, smaller exonic deletions of *SLC20A2* were reported in four patients (31). We identified a ~578 kb deletion in a Finnish family with PFBC using both WGS and a SNP array. The exact breakpoints of the deletion could be identified from the whole genome sequencing data.

The deletion abolishes the first noncoding exon, the 5' UTR region and most likely the promoter region of *SLC20A2* leaving the entire coding region intact. The coding regions of six other genes (*SMIM19*, *CHRNB3*, *CHRNA6*, *THAP1*, *RNF170*, and *HOOK3)* are deleted. At the centromeric breakpoint, the putative promoter region and first two exons of *FNTA* are deleted but the remaining exons are present in two copies (Figure 1c).

The deletion reported by Baker et al. covers the entire coding region of *SLC20A2* and most likely results in reduced expression (25). The exonic deletions reported by David et al. presumably lead to loss of function by removing the translation initiation codon (exon 2 deletion), causing a frameshift (exon 4 deletion) or removing two transmembrane domains (deletion of exons 4 and 5) (31) . The deletion reported here starts between the first two exons of *SLC20A2* removing the noncoding exon 1, 5' UTR and the putative promoter region upstream of the transcription start site. Generally no transcript is produced if the promoter region is missing. We propose that the deletion leads to reduced expression of *SLC20A2* and is thus causative of PFBC in the Finnish family.

Baker et al. reported dystonia in 8 of 11 affected individuals of the family with *SLC20A2* deletion (25). They hypothesized that deletion of *THAP1* might contribute to this as mutations in *THAP1* have been linked to idiopathic torsion dystonia of mixed type (DYT6, OMIM 602629). Interestingly, the youngest patient described here also had cervical dystonia (torticollis spasmodica). The possible phenotypic consequences of the other deleted genes are currently unclear. Genes affected by the deletion code for small integral membrane protein (*SMIM19*), beta and alpha subunits of the neuronal cholinergic nicotinic receptor (*CHRNB3* and *CHRNA1*), endoplasmic reticulum membrane ubiquitin ligase (*RNF170*), cytosolic coiled-coil microtubule binding protein (*HOOK3*), and farnesyltransferase (*FNTA*). Apart from *RNF170*, most of them have not been linked to neurological diseases. A missense mutation (p.Arg199Cys) in *RNF170* has been shown to segregate with autosomal dominant sensory ataxia in two families (36) but, as also noted by Baker et al.(25), the suggested disease-mechanism was gain-of-function. Thus, the possible effects of deletion of one *RNF170* allele are still unknown.

Conclusions

Our results give further support for haploinsufficiency of *SLC20A2* as a pathogenetic route in PFBC and suggest that deletion of regulatory regions of *SLC20A2* is sufficient to cause the disease. The partial deletion of *SLC20A2* described here demonstrates that copy number analysis is essential when screening for mutations in known causative genes in primary familial brain calcification. Ideally, CNV analysis should not be limited to coding regions as causative copy number variations may reside in regulatory regions of known disease-associated genes.

Acknowledgements

The authors thank all the patients and other members of the family for participating in this study.

The authors acknowledge support from Science for Life Laboratory, the Knut and Alice Wallenberg Foundation, the National Genomics Infrastructure funded by the Swedish Research Council, and Uppsala Multidisciplinary Center for Advanced Computational Science for assistance with massively parallel sequencing.

Conflict of interest and sources of funding

All authors declare no conflicts of interest.

This work was supported by Päivikki and Sakari Sohlberg Foundation (PP, LM), Pirkko and Veikko Mäkelä Foundation (PP), the Academy of Finland (LM) and Helsinki University Hospital (MV, LM, PJT and MP). RG and JB are supported by fellowships from the Alzheimer's Society.

WORD COUNT OF THE ARTICLE: 2066 (including the title, 13 words)

References

1. Dai X, Gao Y, Xu Z, Cui X, Liu J, Li Y, et al. Identification of a novel genetic locus on chromosome 8p21.1-q11.23 for idiopathic basal ganglia calcification. Am J Med Genet B Neuropsychiatr Genet. 2010;153B(7):1305-10.
2. Wang C, Li Y, Shi L, Ren J, Patti M, Wang T, et al. Mutations in SLC20A2 link familial idiopathic basal ganglia calcification with phosphate homeostasis. Nat Genet. 2012;44(3):254-6.
3. Manyam BV, Walters AS, Keller IA, Ghobrial M. Parkinsonism associated with autosomal dominant bilateral striopallidodentate calcinosis. Parkinsonism Relat Disord. 2001;7(4):289-95.
4. Hsu SC, Sears RL, Lemos RR, Quintáns B, Huang A, Spiteri E, et al. Mutations in SLC20A2 are a major cause of familial idiopathic basal ganglia calcification. Neurogenetics. 2013;14(1):11-22.
5. Chen WJ, Yao XP, Zhang QJ, Ni W, He J, Li HF, et al. Novel SLC20A2 mutations identified in southern Chinese patients with idiopathic basal ganglia calcification. Gene. 2013;529(1):159-62.
6. Nicolas G, Pottier C, Maltête D, Coutant S, Rovelet-Lecrux A, Legallic S, et al. Mutation of the PDGFRB gene as a cause of idiopathic basal ganglia calcification. Neurology. 2013;80(2):181-7.
7. Keller A, Westenberger A, Sobrido MJ, García-Murias M, Domingo A, Sears RL, et al. Mutations in the gene encoding PDGF-B cause brain calcifications in humans and mice. Nat Genet. 2013;45(9):1077-82.
8. Legati A, Giovannini D, Nicolas G, López-Sánchez U, Quintáns B, Oliveira JR, et al. Mutations in XPR1 cause primary familial brain calcification associated with altered phosphate export. Nat Genet. 2015;47(6):579-81.
9. Miller DG, Edwards RH, Miller AD. Cloning of the cellular receptor for amphotropic murine retroviruses reveals homology to that for gibbon ape leukemia virus. Proc Natl Acad Sci U S A. 1994;91(1):78-82.
10. van Zeijl M, Johann SV, Closs E, Cunningham J, Eddy R, Shows TB, et al. A human amphotropic retrovirus receptor is a second member of the gibbon ape leukemia virus receptor family. Proc Natl Acad Sci U S A. 1994;91(3):1168-72.
11. Kavanaugh MP, Miller DG, Zhang W, Law W, Kozak SL, Kabat D, et al. Cell-surface receptors for gibbon ape leukemia virus and amphotropic murine retrovirus are inducible sodium-dependent phosphate symporters. Proc Natl Acad Sci U S A. 1994;91(15):7071-5.
12. Jensen N, Schrøder HD, Hejbøl EK, Füchtbauer EM, de Oliveira JR, Pedersen L. Loss of function of Slc20a2 associated with familial idiopathic Basal Ganglia calcification in humans causes brain calcifications in mice. J Mol Neurosci. 2013;51(3):994-9.
13. Jensen N, Autzen JK, Pedersen L. Slc20a2 is critical for maintaining a physiologic inorganic phosphate level in cerebrospinal fluid. Neurogenetics. 2016;17(2):125-30.
14. Armulik A, Genové G, Mäe M, Nisancioglu MH, Wallgard E, Niaudet C, et al. Pericytes regulate the blood-brain barrier. Nature. 2010;468(7323):557-61.
15. Daneman R, Zhou L, Kebede AA, Barres BA. Pericytes are required for blood-brain barrier integrity during embryogenesis. Nature. 2010;468(7323):562-6.
16. Giovannini D, Touhami J, Charnet P, Sitbon M, Battini JL. Inorganic phosphate export by the retrovirus receptor XPR1 in metazoans. Cell Rep. 2013;3(6):1866-73.
17. Yamada M, Tanaka M, Takagi M, Kobayashi S, Taguchi Y, Takashima S, et al. Evaluation of SLC20A2 mutations that cause idiopathic basal ganglia calcification in Japan. Neurology. 2014;82(8):705-12.
18. Kasuga K, Konno T, Saito K, Ishihara A, Nishizawa M, Ikeuchi T. A Japanese family with idiopathic basal ganglia calcification with novel SLC20A2 mutation presenting with late-onset hallucination and delusion. J Neurol. 2014;261(1):242-4.
19. Nicolas G, Pottier C, Charbonnier C, Guyant-Maréchal L, Le Ber I, Pariente J, et al. Phenotypic spectrum of probable and genetically-confirmed idiopathic basal ganglia calcification. Brain. 2013;136(Pt 11):3395-407.

20. Lemos RR, Ramos EM, Legati A, Nicolas G, Jenkinson EM, Livingston JH, et al. Update and Mutational Analysis of SLC20A2: A Major Cause of Primary Familial Brain Calcification. Hum Mutat. 2015;36(5):489-95.
21. Taglia I, Mignarri A, Olgiati S, Menci E, Petrocelli PL, Breedveld GJ, et al. Primary familial brain calcification: Genetic analysis and clinical spectrum. Mov Disord. 2014;29(13):1691-5.
22. Lemos RR, Oliveira MF, Oliveira JR. Reporting a new mutation at the SLC20A2 gene in familial idiopathic basal ganglia calcification. Eur J Neurol. 2013;20(3):e43-4.
23. Brighina L, Saracchi E, Ferri F, Gagliardi M, Tarantino P, Morzenti S, et al. Fahr's disease linked to a novel SLC20A2 gene mutation manifesting with dynamic aphasia. Neurodegener Dis. 2014;14(3):133-8.
24. Liu X, Ma G, Zhao Z, Mao F, Tang J, Li X, et al. Novel mutation of SLC20A2 in a Chinese family with primary familial brain calcification. J Neurol Sci. 2016;360:1-3.
25. Baker M, Strongosky AJ, Sanchez-Contreras MY, Yang S, Ferguson W, Calne DB, et al. SLC20A2 and THAP1 deletion in familial basal ganglia calcification with dystonia. Neurogenetics. 2014;15(1):23-30.
26. Ferreira JB, Pimentel L, Keasey MP, Lemos RR, Santos LM, Oliveira MF, et al. First report of a de novo mutation at SLC20A2 in a patient with brain calcification. J Mol Neurosci. 2014;54(4):748-51.
27. Gagliardi M, Morelli M, Annesi G, Nicoletti G, Perrotta P, Pustorino G, et al. A new SLC20A2 mutation identified in southern Italy family with primary familial brain calcification. Gene. 2015;568(1):109-11.
28. Zhang Y, Guo X, Wu A. Association between a novel mutation in SLC20A2 and familial idiopathic basal ganglia calcification. PLoS One. 2013;8(2):e57060.
29. Zhu M, Zhu X, Wan H, Hong D. Familial IBGC caused by SLC20A2 mutation presenting as paroxysmal kinesigenic dyskinesia. Parkinsonism Relat Disord. 2014;20(3):353-4.
30. Rubino E, Giorgio E, Gallone S, Pinessi L, Orsi L, Gentile S, et al. Novel mutation of SLC20A2 in an Italian patient presenting with migraine. J Neurol. 2014;261(10):2019-21.
31. David S, Ferreira J, Quenez O, Rovelet-Lecrux A, Richard AC, Vérin M, et al. Identification of partial SLC20A2 deletions in primary brain calcification using whole-exome sequencing. Eur J Hum Genet. 2016.
32. Wang K, Li M, Hakonarson H. ANNOVAR: functional annotation of genetic variants from high-throughput sequencing data. Nucleic Acids Res. 2010;38(16):e164.
33. Cingolani P, Platts A, Wang lL, Coon M, Nguyen T, Wang L, et al. A program for annotating and predicting the effects of single nucleotide polymorphisms, SnpEff: SNPs in the genome of Drosophila melanogaster strain w1118; iso-2; iso-3. Fly (Austin). 2012;6(2):80-92.
34. Klambauer G, Schwarzbauer K, Mayr A, Clevert DA, Mitterecker A, Bodenhofer U, et al. cn.MOPS: mixture of Poissons for discovering copy number variations in next-generation sequencing data with a low false discovery rate. Nucleic Acids Res. 2012;40(9):e69.
35. Nicolas G, Rovelet-Lecrux A, Pottier C, Martinaud O, Wallon D, Vernier L, et al. PDGFB partial deletion: a new, rare mechanism causing brain calcification with leukoencephalopathy. J Mol Neurosci. 2014;53(2):171-5.
36. Valdmanis PN, Dupré N, Lachance M, Stochmanski SJ, Belzil VV, Dion PA, et al. A mutation in the RNF170 gene causes autosomal dominant sensory ataxia. Brain. 2011;134(Pt 2):602-7.
37. Robinson JT, Thorvaldsdóttir H, Winckler W, Guttman M, Lander ES, Getz G, et al. Integrative genomics viewer. Nat Biotechnol. 2011;29(1):24-6.
38. Thorvaldsdóttir H, Robinson JT, Mesirov JP. Integrative Genomics Viewer (IGV): high-performance genomics data visualization and exploration. Brief Bioinform. 2013;14(2):178-92.

355 **Titles and legends to figures**

356 **Figure 1. (a)** Brain CT of patient II:2 showing calcification (marked with arrows) in basal
357 ganglia and cerebellum. **(b)** Pedigree of the family with screenshots of SNP array data and
358 the deletion breakpoint in *SLC20A2* in WGS data visualized using the Integrative Genomics
359 Viewer (IGV) (37, 38). Circles mark females, squares males. Affected persons are marked by
360 a filled symbol and deceased persons with a slashed symbol. DNA samples were available
361 from persons marked with an asterisk. **(c)** Schematic drawing of the deletion area on 8p11.2.
362 The deletion reported by Baker et al. (25) is shown for comparison. Orientations of the genes
363 are marked with arrows.

364

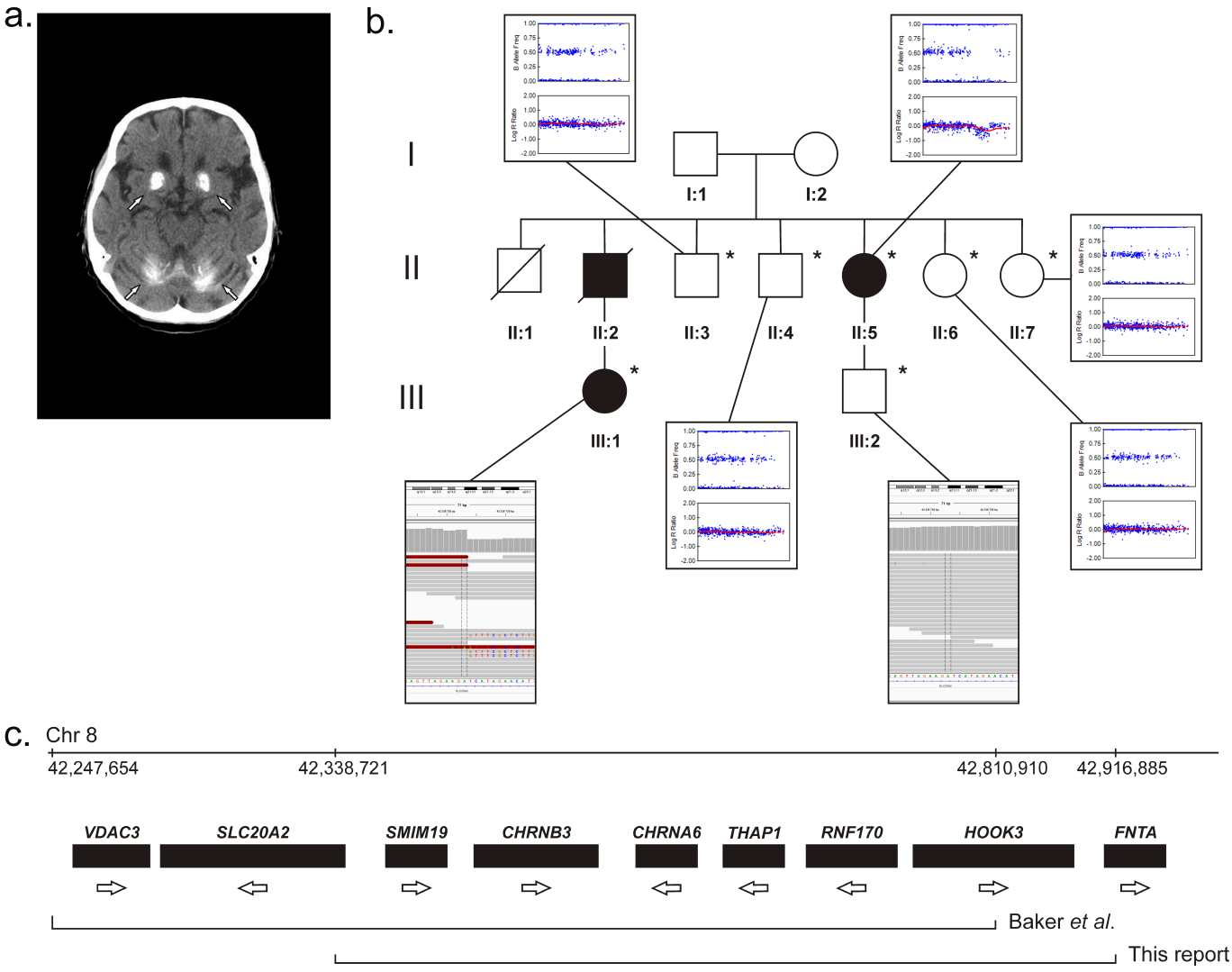
a.
b.
I
II
III
I:1
I:2
II:1
II:2
II:3
II:4
II:5
II:6
II:7
III:1
III:2
c.
Chr 8
42,247,654
42,338,721
42,810,910
42,916,885
VDAC3
SLC20A2
SMIM19
CHRNB3
CHRNA6
THAP1
RNF170
HOOK3
FNTA
Baker et al.
This report

Supplementary table 1. WGS analysis results showing the presence of heterozygous deletion affecting SLC20A2 in PFBC patient's sample (grey-shaded columns).

1a. cn.mops analysis results from the deletion area (CN2 indicates two copies and CN1 one copy of a genomic segment).

CHROM	START	END	WIDTH	Reference_sample 1	Reference sample_2	PFBC_sample	PFBC_control	GENE
8	42339001	42429000	90000	CN2	CN2	CN1	CN2	SLC20A2;SMIM19
8	42431001	42543000	112000	CN2	CN2	CN1	CN2	
8	42546001	42799000	253000	CN2	CN2	CN1	CN2	CHRNB3;CHRNA6;THAP1;RNF170;MIR4469;HOOK3
8	42800001	42813000	13000	CN2	CN2	CN1	CN2	HOOK3
8	42816001	42843000	27000	CN2	CN2	CN1	CN2	HOOK3
8	42844001	42877000	33000	CN2	CN2	CN1	CN2	HOOK3
8	42878001	42917000	39000	CN2	CN2	CN1	CN2	HOOK3;FNTA

1b. Manta analysis results from the deletion area (0/1 indicates heterozygous deletion, 0/0 indicates wild type).

CHROM	POS	ID	REF	ALT	FILTER	INFO	PFBC_sample	PFBC_control	Reference_sample1	Reference_sample2
8	42338721	MantaDEL:159946	A	<DEL>	PASS	END=42916885	0/1:PASS	0/0:PASS	0/0:PASS	0/0:PASS

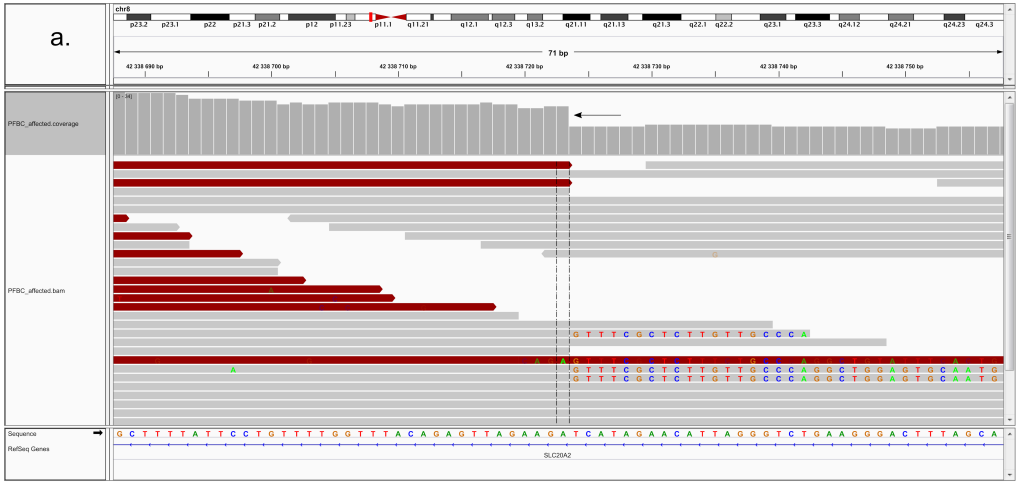
a.
chr8
71 bp
PFBC_affected.coverage
PFBC_affected.bam
Sequence
RefSeq Genes
SLC20A2

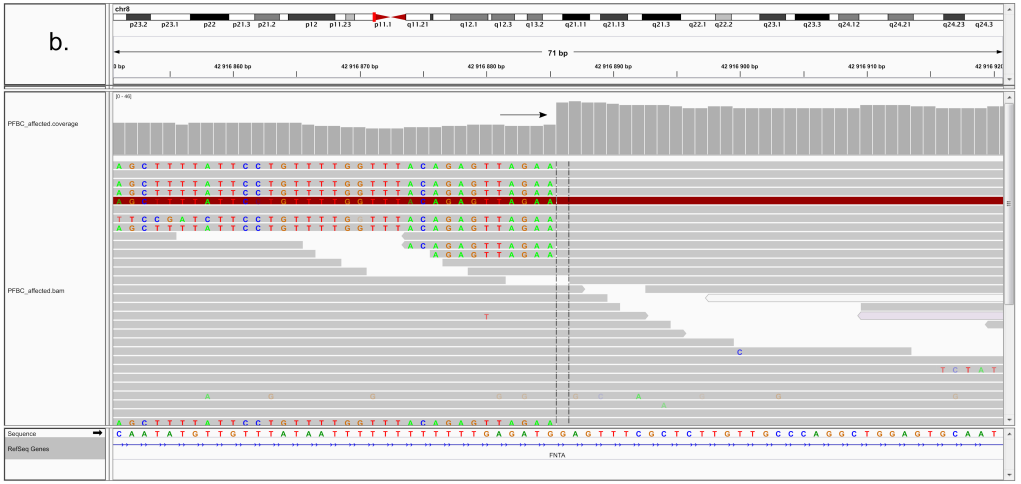
b.
chr8
71 bp
PFBC_affected.coverage
PFBC_affected.bam
Sequence
RefSeq Genes
FNTA

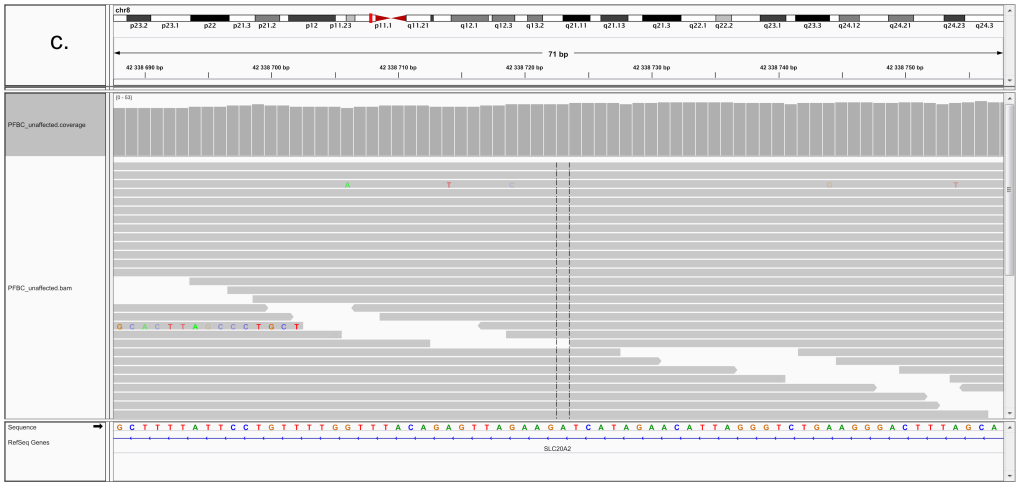
c.
chr8
71 bp
PFBC_unaffected.coverage
PFBC_unaffected.bam
Sequence
RefSeq Genes
SLC20A2

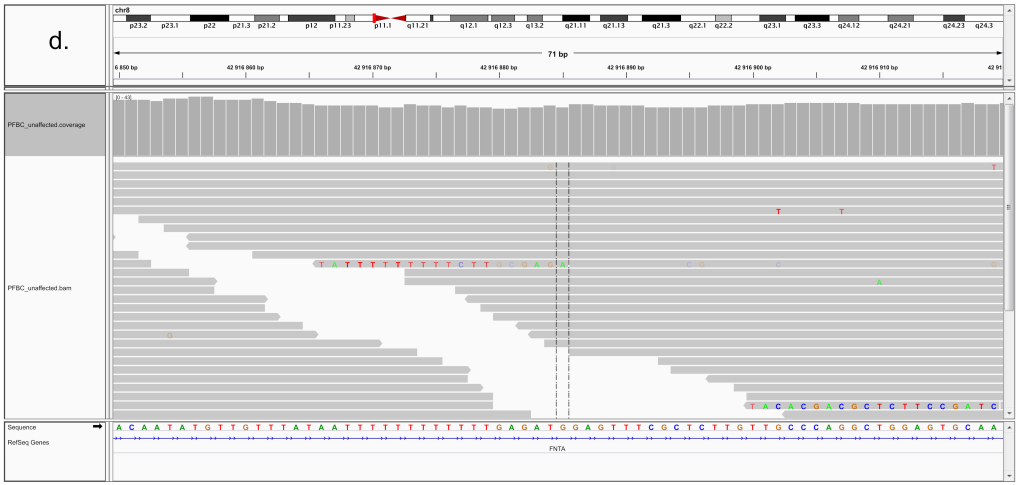
d.
chr8
71 bp
PFBC_unaffected.coverage
PFBC_unaffected.bam
Sequence
RefSeq Genes
FNTA


a.
B Allele Freq
Log R Ratio
II:5
8
Base Position
Cytogenetic Band
Sequence (+)
No sequence data file found for this chromosome.
b.
II:3
c.
II:4
d.
II:6
e.
II:7